Supporting Information

Anisotropically Functionalized Aptamer-DNA Nanostructures for Enhanced Cell Proliferation and Target-Specific Adhesion in 3D Cell Cultures

*Keonwook Nam,† Byeol I Im,† Taehyung Kim, Young Min Kim, and Young Hoon Roh**

Department of Biotechnology, College of Life Science and Biotechnology, Yonsei University, 50 Yonsei-ro, Seodaemun-gu, Seoul 03722, Republic of Korea.

Corresponding Author

*Email: yr36@yonsei.ac.kr

Table S1. Oligonucleotide sequences of Apt-X-DNA nanostructures.[a]

Strand	Sequence (5' – 3')	ΔG at 60°C (kcal/mol)	T_m (°C)
X1	CGA CCG ATG AAT AGC GGT CAG ATC CGT ACC TAC TCG	0.4	54.7
X2	CGA GTA GGT ACG GAT CTG CGT ATT GCG AAC GAC TCG	0.87	47.5
X3	CGA GTC GTT CGC AAT ACG GCT GTA CGT ATG GTC TCG	1.29	48.6
X4	CGA GAC CAT ACG TAC AGC ACC GCT ATT CAT CGG TCG	0.59	51.7
AS1411-T(n)-X1	GGT GGT GGT GGT TGT GGT GGT GGT GG T(n) CGA CCG ATG AAT AGC GGT CAG ATC CGT ACC TAC TCG	0.4	54.7
AS1411-T(n)-X2	GGT GGT GGT GGT TGT GGT GGT GGT GG T(n) CGA GTA GGT ACG GAT CTG CGT ATT GCG AAC GAC TCG	0.87	47.5
AS1411-T(n)-X3	GGT GGT GGT GGT TGT GGT GGT GGT GG T(n) CGA GTC GTT CGC AAT ACG GCT GTA CGT ATG GTC TCG	1.29	48.6

[a]Note: Anti-nucleolin aptamer (AS1411) sequences are underlined.

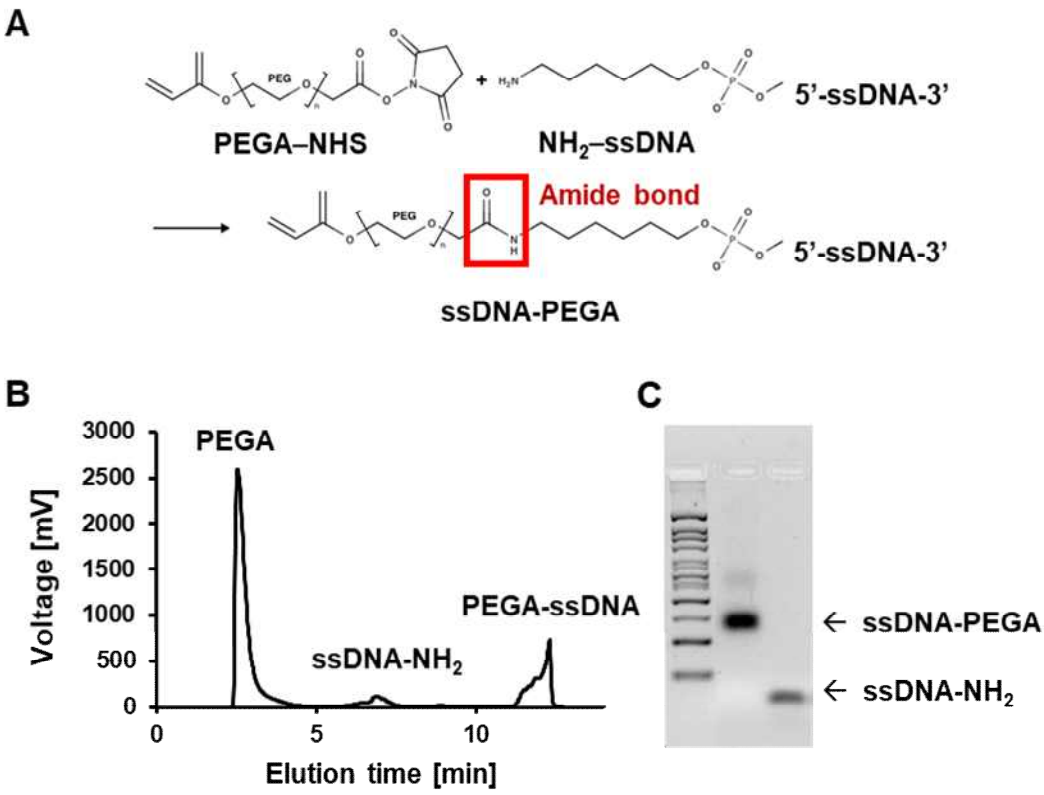

Figure S1. Synthesis and purification of photo-crosslinkable ssDNA-PEGA. (A) Schematic diagram of ssDNA-NH2 pegylation via NHS ester reaction to form an amide bond. (B) HPLC chromatogram of PEGA-conjugated ssDNA and residual products. (C) Verification of the separation and purification of ssDNA-PEGA via gel electrophoresis. ssDNA-PEGA is represented in Lane 1 and ssDNA-NH2 is represented in Lane 2.

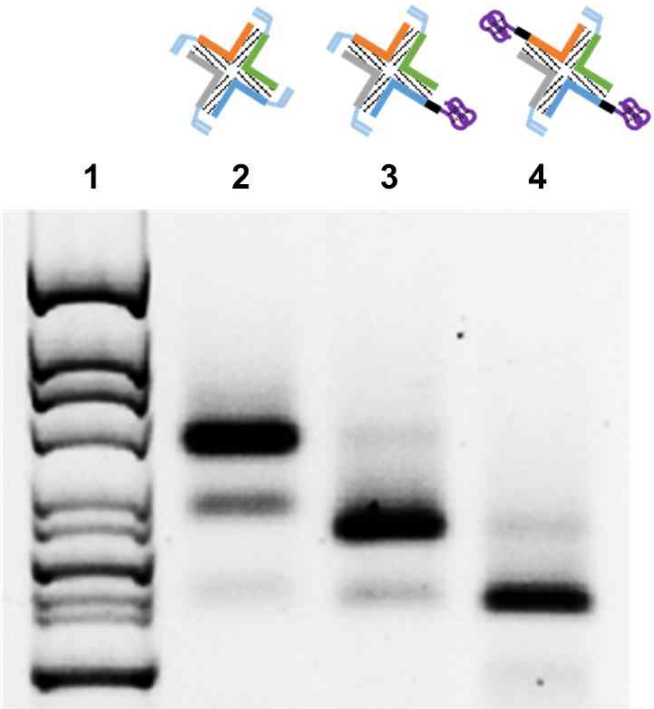

Figure S2. Gel electrophoresis of aptamer-functionalized X-DNA. Lane 1: ladder; lane 2: Apt-X (0); lane 3: Apt-X (1); lane 4: Apt-X (2).

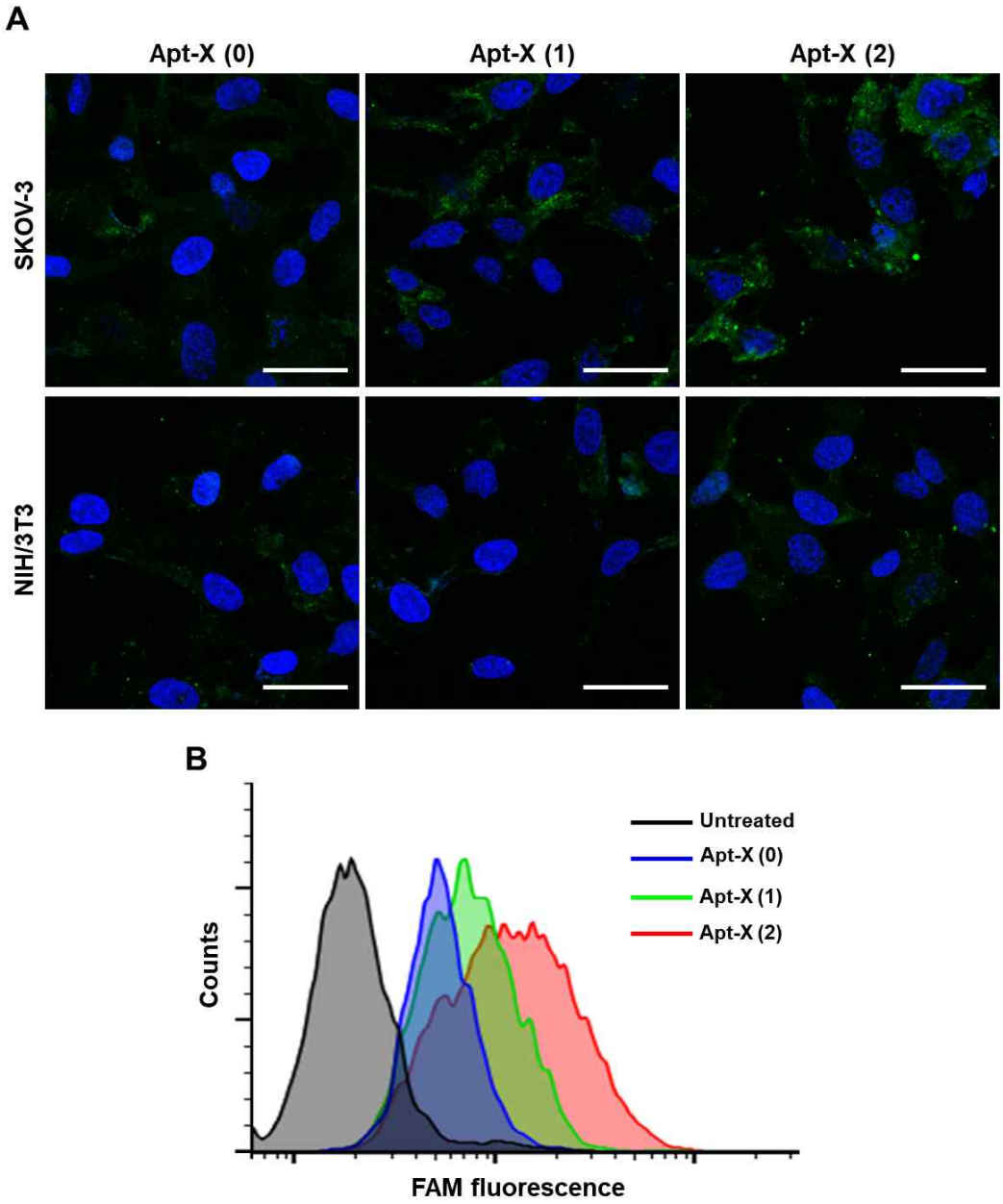

Figure S3. Verification of aptamer number-dependent cell surface interaction of Apt-X -DNA nanostructures. (A) CLSM and (B) Flow cytometry analysis of NIH/3T3 and SKOV-3 cells that were treated with FAM-labeled Apt-X (0), Apt-X (1), and Apt-X (2). Scale bar: 20 μm.

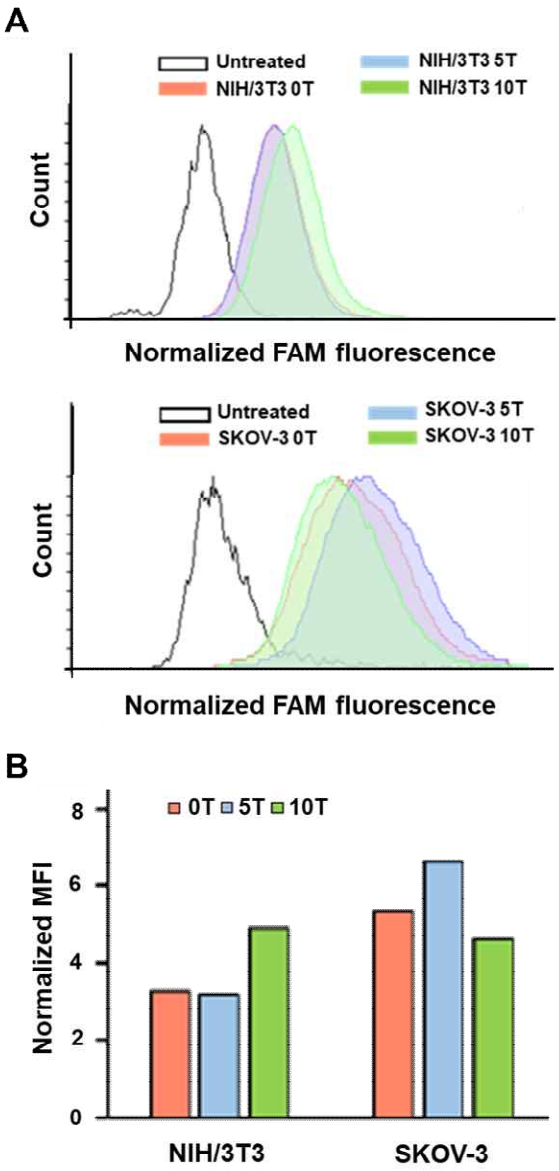

Figure S4. **Analysis of spacer number-dependent cellular interaction.** (A) Flow cytometry analysis and (B) normalized mean fluorescence intensity (MFI) of NIH/3T3 and SKOV-3 cells that were treated with FAM-labeled Apt-X (2) with 0, 5-, and 10-nucleotide-long spacer sequences.

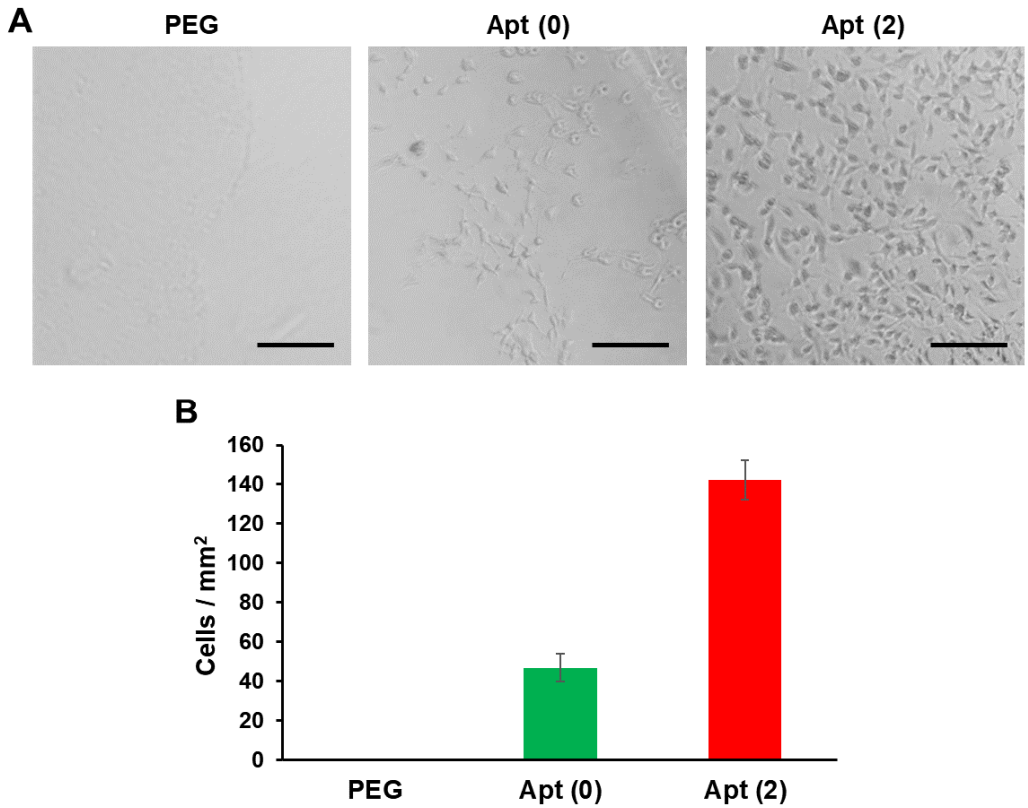

Figure S5. Comparison of cell adhesion of DNA hybrid hydrogels. (A) Contrast-enhanced light microscopy images and (B) quantification by ImageJ analysis of PEG, Apt (0), and Apt (2) hydrogels that were synthesized with 100 pmol of Apt-X-DNA and were incubated for 3 h in cell media with 2.5 × 10^4 SKOV-3 cells. Scale bar: 0.2 mm.

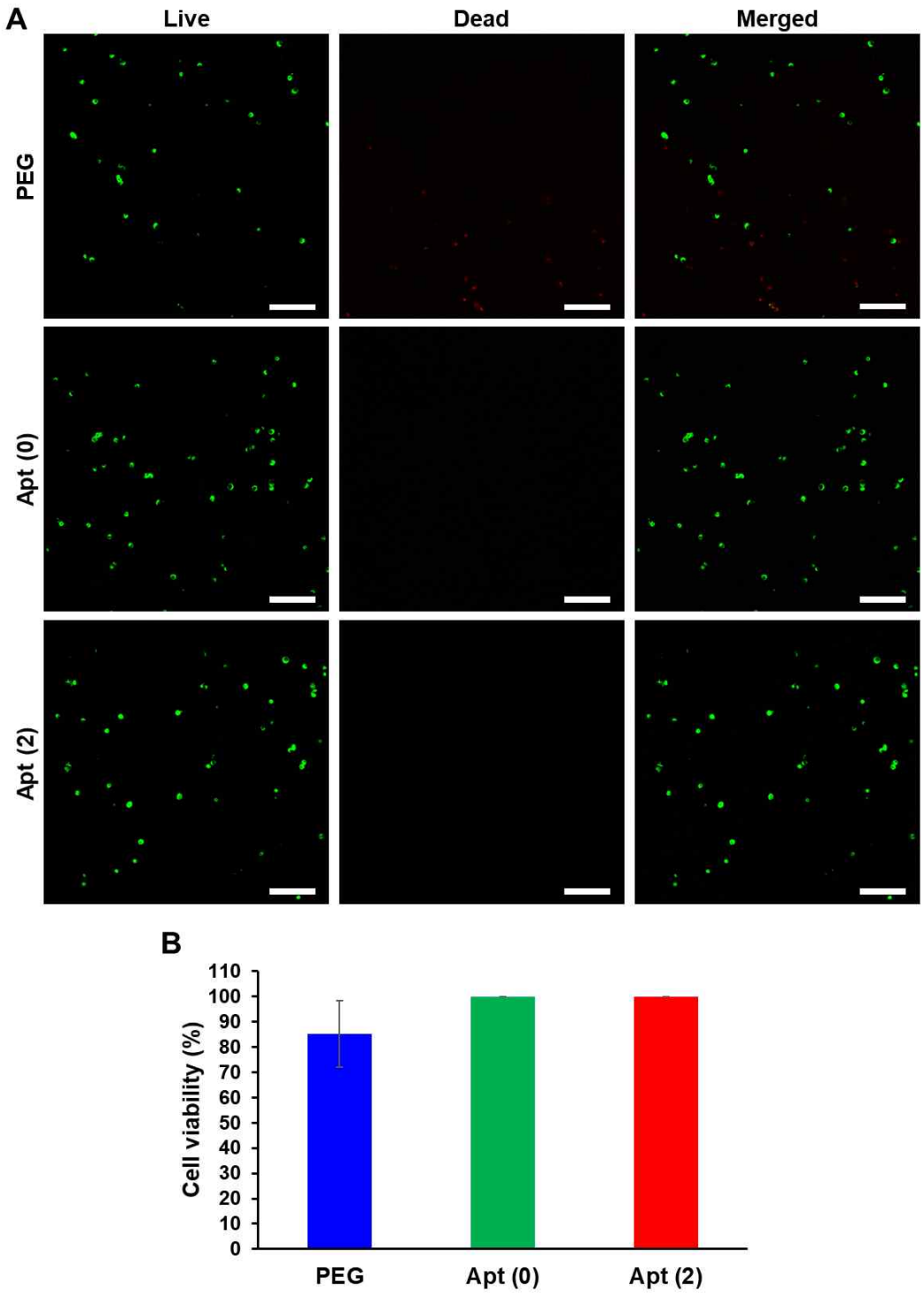

Figure S6. Cytotoxicity evaluation of photo-crosslinking reaction. (A) Live/dead assay of PEG, Apt (0), and Apt (2) hydrogels photo-polymerized with 100 pmol of Apt-X-DNA and 1×10^4 SKOV-3 cells after 1 day of culture observed with confocal laser scanning microscopy. Scale bar: 10 μm. (B) Quantitative analysis of CLSM images with ImageJ.

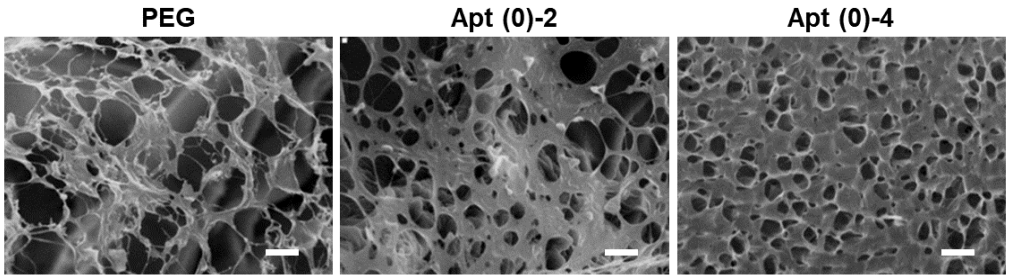

Figure S7. Structural characterization of DNA hybrid hydrogels. SEM analysis of hydrogels synthesized with 0, 2, and 4 nmol of Apt-X (0) to investigate the effect of varying the concentration of Apt-X-DNA nanostructure on porosity of the hydrogels. Scale bar: 10 μm.

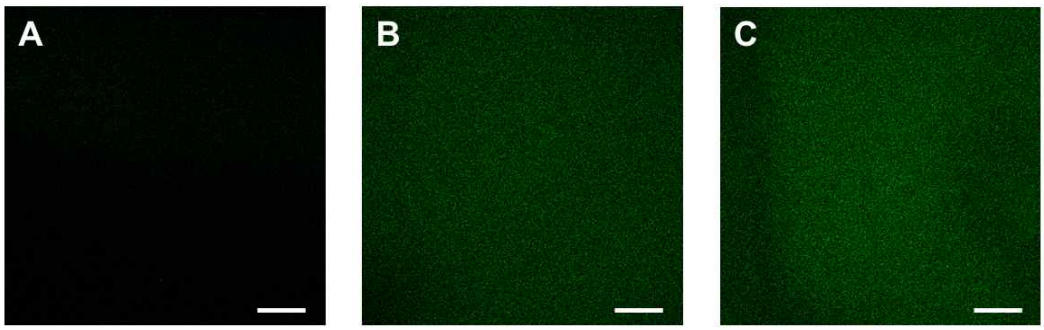

Figure S8. Verification of the presence of DNA in hydrogels. CLSM analysis of hydrogels photo-crosslinked with (A) 1 nmol, (B) 2 nmol, and (C) 4 nmol of SYBR-intercalated Apt-X (0). Scale bar: 20 μm.

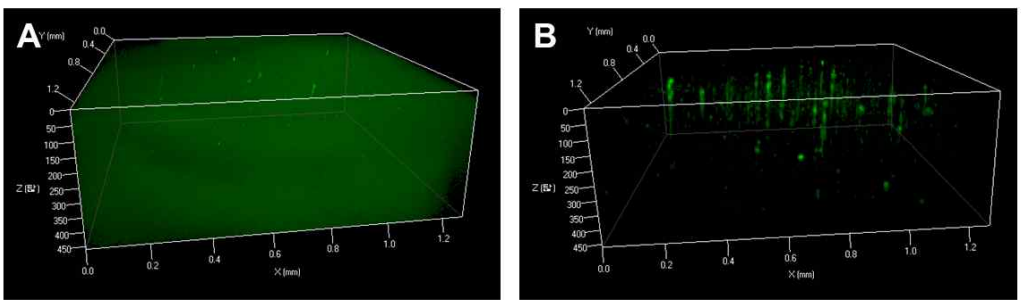

Figure S9. Verification of the photo-polymerization of DNA in hydrogels. CLSM analysis of hydrogels photo-crosslinked with 100 pmol of SYBR-intercalated (A) Apt-X (0) and (B) blunt X-DNA.

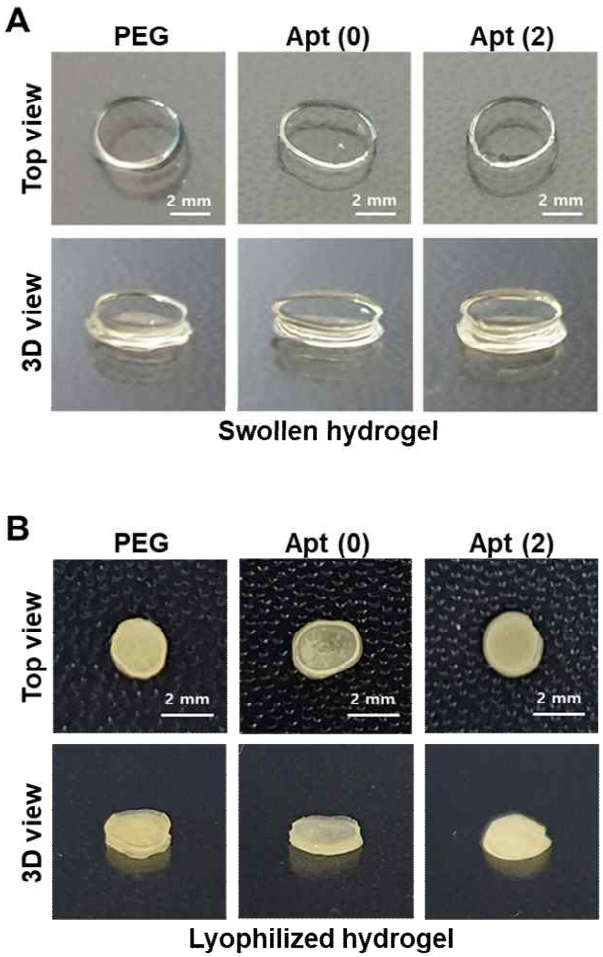

Figure S10. Confirmation of photo-polymerization of DNA hybrid hydrogels. Digital images of (A) swollen and (B) lyophilized DNA hybrid hydrogels.

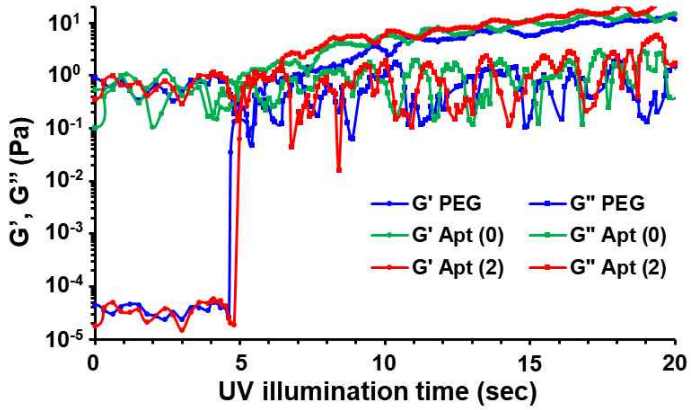

Figure S11. Comparison of the gelation rate of DNA hybrid hydrogels. Change in storage (G′) and loss (G″) modulus of PEG, Apt (0), and Apt (2) hydrogel precursor solutions over time upon illumination of UV wavelength of 365 nm.

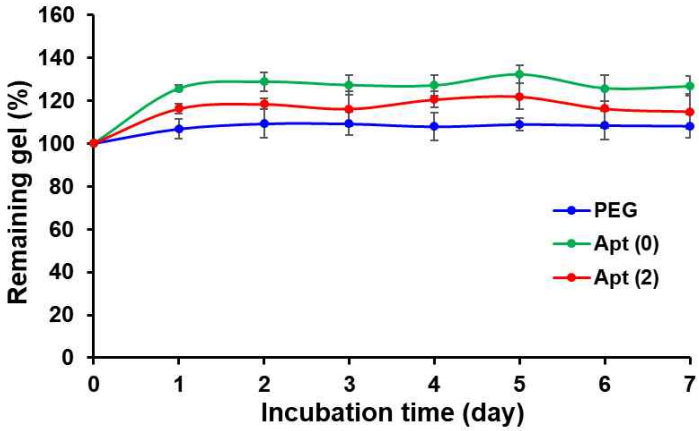

Figure S12. Degradation profiles of DNA hybrid hydrogels. PEG, Apt (0), and Apt (2) hydrogels were incubated in cell culture media for seven days. 'Remaining gel %' refers to the percentage change in mass remaining from the starting gels. The error bars represent standard deviation of at least three replicates.

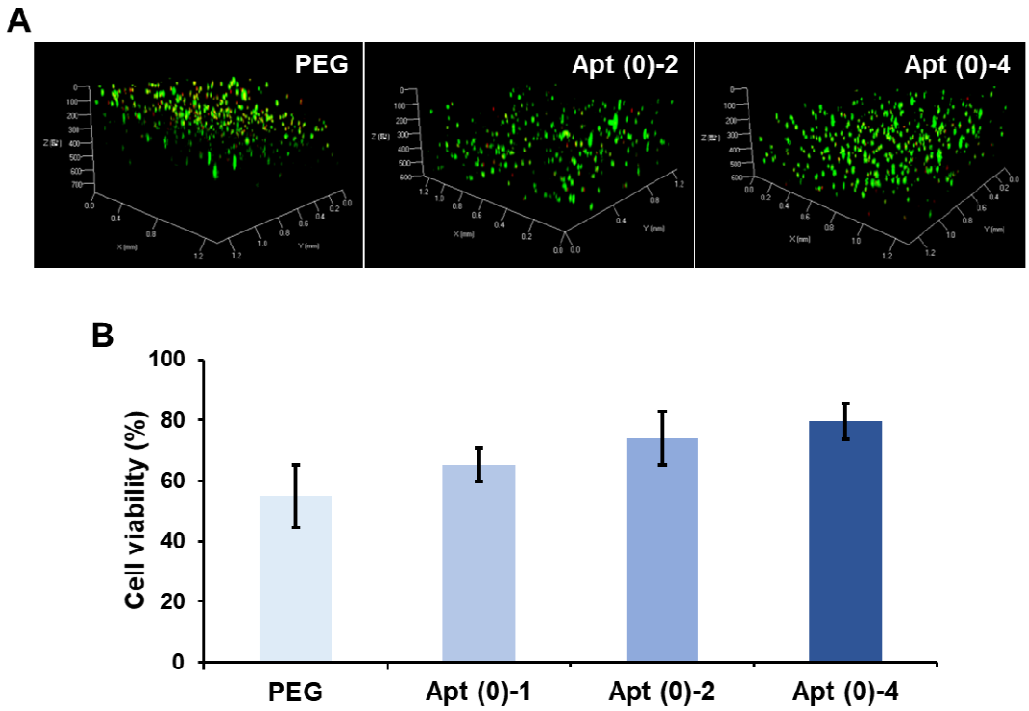

Figure S13. Effect of Apt-X-DNA nanostructure concentration on cell viability. (A) Live/dead 3D representations and (B) cell viability calculated by ImageJ analysis of PEG, Apt (0)-2, and Apt (0)-4 hydrogels after culturing 3×10^3 SKOV-3 cells for seven days.